Research Article

Rusal S. Huissen* and Bushra. S. Albusoda

Behavior of group piles under combined loadings after improvement of liquefiable soil with nanomaterials

https://doi.org/10.1515/jmbm-2022-0059
received March 20, 2022; accepted May 15, 2022

Abstract: Earthquake-induced liquefaction is prone in a region with loosely saturated sand and higher seismic activity. In recent years, improvement techniques have been used as a pre-construction or retrofitting method for the current construction. Several methods are intended as remedial techniques, which include either densifying the deposit soil, inserting a unique material, or controlling dissipated pore water pressure generated during the seismic motion. The permeation grouting technique is primarily used in remedial liquefaction schemes that aim to improve the soil deposit mainly by cementing the soil particles and filling the void spaces, thereby preventing soil disturbance caused by settlements or distress to an existing foundation or structure. Permeation grouting involves the injection of a low viscosity chemical or particulate grout into the soil pores with little to no change in the soil structure and has been shown to be effective at reducing liquefaction risk beneath existing structures in soils where it is applicable. The mitigation of liquefaction risk by incorporating nanomaterials using the permeation grouting technique, to study the performance of a pile group embedded in the liquefiable treated layer with 1/50 nano-clay and 1/30 nano-SiO_2 after 48 h of curing time during the Kobe earthquake, has been adopted. The soil profile treated using nanomaterials showed that the soil stiffness and strength were preserved during shaking because it did not liquefy; simultaneously, the maximum pile bending moments and lateral pile displacements in the treated soil layer were reduced by 30%. Finally, after treatment, the nanomaterials have a significant effect on the reduction of the maximum accelerations in two depths of soil.

Keywords: permeation grouting, nano-SiO_2, nano-clay, Kobe earthquake, pile group, SEM, X-ray, liquefiable soil

1 Introduction

Nanomaterials are a new material level between atoms, molecules, and macroscopic materials with at least one spatial dimension that does not exceed 100 nm. Nanomaterials have a higher specific surface area than their volume, leading to much water encompassing the outer surface. The existence of those materials in soil usually enhances its thixotropic property and increases its shear strength. These materials can be used by reducing the possibility of liquefaction with hydraulic fills or saturated fine sand [1]. Many different types and methods of mitigation were found and suggested for use depending on many factors. The highlights must be focused on ground mitigation, and improvement techniques must be sustainable, keep time, and be cost-effective. The current research focuses on one of the sites containing civilian pile foundations of existing buildings; thus, the target is for mitigation methods that satisfy this condition. During liquefaction, the lateral resistance decreases, whereas the lateral deformation (buckling failure) increases [2]. The liquefaction potential can be reduced by increasing the shear strength and the densification extent. Grouting can be used in constrained sites; traditional grouting materials include cement slurry, sodium silica, and chemical grouts. The chemical grouting method has a high risk of damage to adjacent buildings and pollution of waterways; therefore, with increased industrialization and urbanization and the progress of creative science and technology, alternative materials for mitigating liquefaction risks should be explored [3]. Currently, nanoparticles have been used for stabilizing instead of applying traditional materials; these materials impact physical, chemical, and engineering properties. Hence, using permeation grouting with nanomaterials as a novel liquefaction

* **Corresponding author: Rusal S. Huissen,** Civil Engineering Department, Civil Engineering, Al-Farabi University, Baghdad, Iraq, e-mail: Salamrusal@gmail.com
Bushra. S. Albusoda: Civil Engineering Department, Civil Engineering, University of Baghdad, Baghdad, Iraq, e-mail: dr.bushra_albusoda@coeng.uobaghdad.edu.iq

mitigation method, this method does not cause ground disturbance and can be treated over the entire site. Çelik *et al.* [4] studied the effects of two types of nanomaterials (nano-aluminum and nanosilica) on the strength properties of poorly graded sand under different percentages of water injected into the sandy soil with a relative density of 70% and a pressure of 2 bars for 7 and 28 days as curing time. It can be concluded that the compressive strength increases with the addition of nanoparticles up to a certain point and stops after a particular point. The liquefaction mitigation methods are dependent on many principles, including densification, reinforcement, and accelerated saturated soil drainage during earthquake motions and other processes. Liquefaction mitigation in the urban area is very complex and has many limitations [5]. Thus, in this study, the focus is to use non-destructive methods in the mitigation process. Permeation grouting with nanomaterials in a horizontal direction is one of the mitigation processes to improve the liquefied soil surrounding the pile foundations. The improvement method occurs by changing the soil skeleton and behavior during liquefaction triggering.

2 Materials used

The sandy soil that was used in this study is classified as poorly graded sand (SP) according to the Unified Soil Classification System (ASTM D2487). The grain size distribution curve of this soil is shown in Figure 1. Two types of nanomaterials (nano-SiO_2 and nano-clay) were used. Tables 1 and 2 show the properties of these materials.

The X-ray diffraction analysis of natural and treated sand soil is important for determining changes in the mineralogical composition of the soil as a result of determining whether or not there is a chemical reaction for nanomaterials with sand soil. The curves in Figure 2 included the natural sandy soil, (1/30) nano-clay, and (1/50) nano-SiO_2 obtained from the X-ray test. The intensity of the sand soil mineral peaks decreased slightly because of the used nanomaterials on the sulfate present in the soil, which led to a decrease in the amount of liquefied sand [6]. The X-ray test results given in Figure 2 display the same patterns for the natural and treated sandy soil; this is normal due to the addition of calcium chloride, which is a support reagent that provides calcium, which in turn combines with the carbonates from the hydrolysis to form calcium carbonate. The most prominent clay minerals are calcite, as it was observed that the use in the treatment led to increased calcite precipitation in the sand soil

Table 1: Physical properties of nano-SiO_2 and nano-clay

Properties	Values	
	Nano-SiO_2	Nano-clay
Color	White	Pale yellow
Physical form	Powder	
Density (gm/cm^3)	0.1<	0.5–0.7
Particle size (nm)	11–12	1–2
Specific surface area (cm^2/g)	200	220–270
Specific gravity	2.4–3	3–3.7
Humidity (%)	—	1–2

Table 2: Chemical composition of nano-clay and nano-SiO_2 (according to the table)

Nano-clay		Nano-SiO_2	
Oxide composition	Content (%)	Oxide composition	Content (%)
Na_2O	0.98	SiO_2	99.75
CaO	4.08	Al_2O_3	0.048
K_2O	2.56	Na_2O	0.05
SiO_2	50.14	Fe_2O_3	0.002
Al_2O_3	13.10	K_2O	0.020
MgO	4.78	MgO	0.080
Fe_2O_3	8.80	TiO_2	0.030
TiO_2	0.51	HCl	0.020
Loss on ignition	13.05	—	—

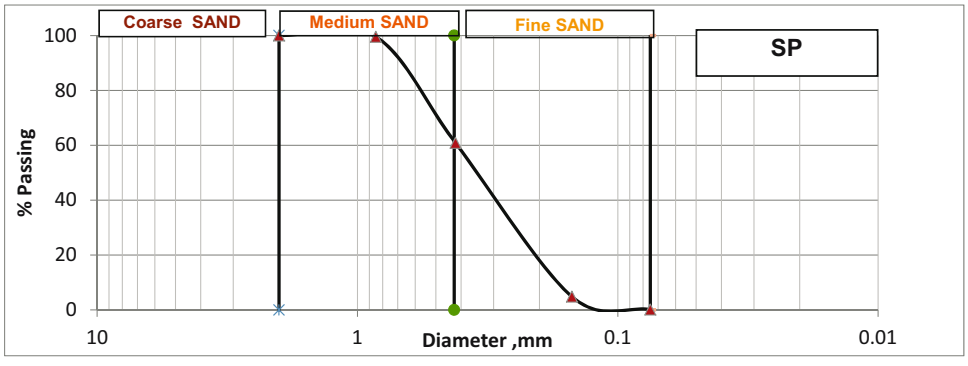

Figure 1: Grain size distribution curve.

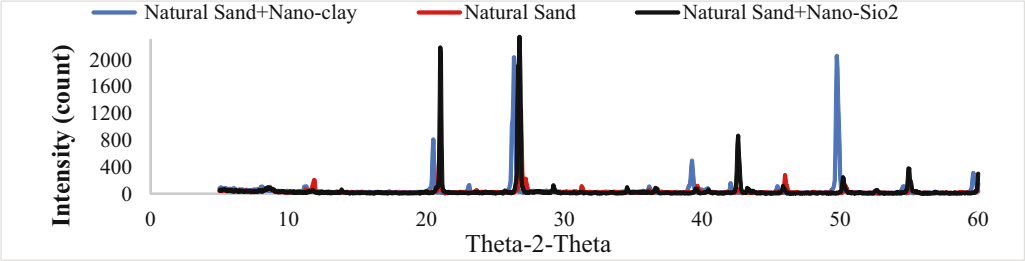

Figure 2: X-ray analysis of sand treated with nano-clay and nano-SiO_2.

samples. Diffraction analysis of treated soil is important to determine the changes that occur in the mineralogical phase reactions. These reactions depend on the chemical and mineralogical composition of each soil and additive. Quartz X-ray diffraction (XRD) peaks are slightly higher than other mineral peaks because quartz spreads X-rays better than other substances. The peak was identified as quartz at 2-Theta 20.9°. The intensity for sand soil before and after treatment with nanomaterials is shown in Table 3; the intensity increased slightly, reflecting the effect of the nanomaterial's existence on the sandy soil. These strength changes again emphasized the influence of the added nanomaterials. As compared to untreated soils, nanomaterial-treated soils show many new peaks. The fact that the chemical action of the nanomaterials was approved with the results found from the strength test may explain this result.

This involves injecting a grout that permeates the surrounding soil pore space before the grout begins to harden or set. The hardened grout improves the soil by cementing the soil particles together and filling the void space [7]. This primary advantage prevents disturbing the native soil due to associated settlements or distress to an existing foundation or structure. The permeation technique includes grouting nanomaterials (gel–solid) into saturated loosely sandy soil using a permeation time and rate. For this purpose, grouting machine-cell equipment that activated seepage through soil strata of sand was used for grouting the gel nanomaterials. The permeation grouting technique includes grouting nanomaterials (gel–solid) into saturated loosely sandy soil using a permeation time and rate. For this purpose, grouting machine-cell equipment that activated seepage through soil strata of sand was used for grouting the gel nanomaterials. It is locally manufactured from ductile steel to resist high pressure with a grouting cell that connects to the air pressure compressor to permit the grouting materials in the cell tube through a pumping hose. The permeation grouting device was manufactured by AL-Kinani [8]. The gel-like solid was injected into sandy soil strata in a laminar soil box to a specific zone depth of loosely saturated sandy soil with a pressure level of 1.2 psi with a curing time of 48 h and nanomaterial ratios of 1/50 and 1/30 for nano-SiO_2 and nano-clay, respectively, through plastic pipes of 3 mm placed in different locations in the horizontal direction of the loosely saturated layer. The overall observations for soil mitigation based on permeation grouting using nanomaterials were assessed by the pore pressure generation, lateral and vertical displacements, acceleration, and bending moments along the pile depth during the Kobe earthquake. Sensors (*e.g.*, accelerometers, ACC2 and ACC3; pore water pressure ratios, ru1 and ru2; lateral and vertical displacement transducers; and strain gauges in the first and second rows of piles, P1 and P2) were used in this study to record various parameters during shaking table tests. The piles were located at a height of 100 mm above the sandy soil surface. Hence, the total pile length is 500 mm. The total allowable axial load capacity was applied by placing the weight block directly on the pile cap. In order to simulate the lateral loading system on the pile head, an automated pneumatic-vacuum loading system was locally manufactured [9,10]. The total allowable lateral load capacity equals 20% of the total allowable axial load. In this study, eight test cases were considered in the shaking table model. In G-1-K and G-2-K case tests, a pure axial load was applied to the pile, whereas the other test cases included combined (axial and lateral) loadings (G-1-2-K and G-2-2-K) through two types of nanomaterials. Figure 3 shows all details of the setup model.

Table 3: Intensity values of different soils obtained for the quartz peak

Natural sand soil	Natural sand + nano-SiO_2	Natural sand + nano-clay
440	2,184	884

3 Results and discussion

Figure 4 shows pile cap displacement in both directions, and the first impression to be noted here is that the lateral

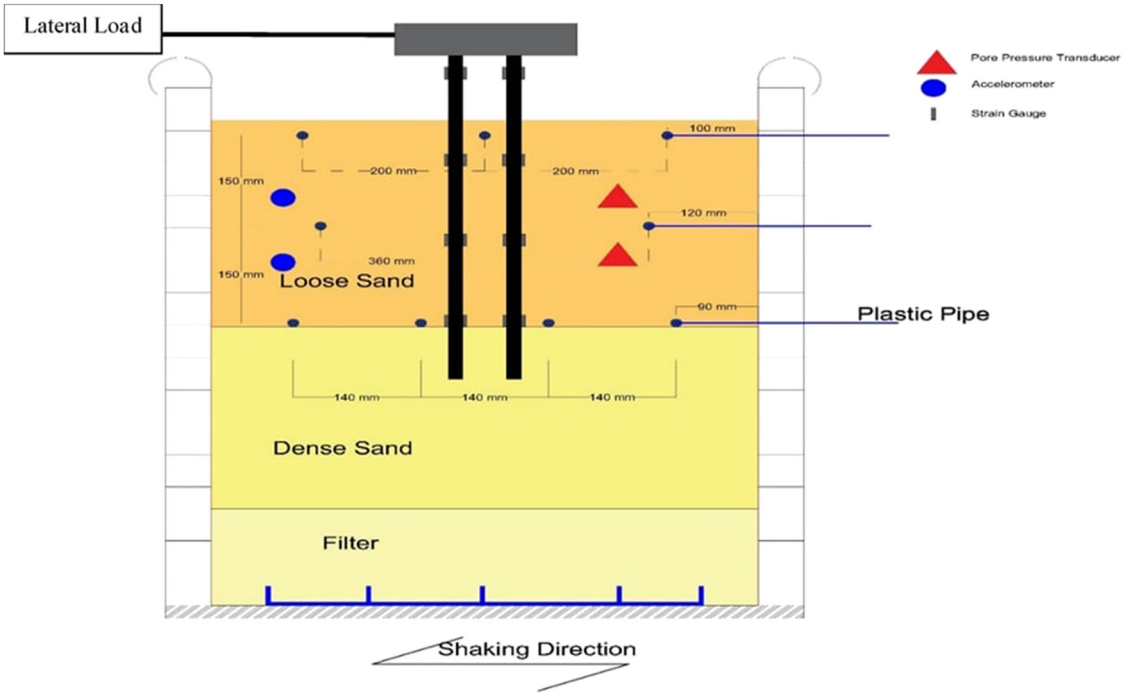

Figure 3: Setup model.

displacement is improved with the use of nano-clay when subjected to strong motion as well as the lateral loading effect, with 100% lateral loading and 50–100% axial loading. When compared to untreated soil, the lateral displacement of the pile cap will be reduced by about 20% for all test cases: G-1-K, G-1-2-K, G-2-K, and G-2-2-K. On the other hand, increasing cap masses by 50% axial for treated cases G-1-K and G-1-2-K will reduce the

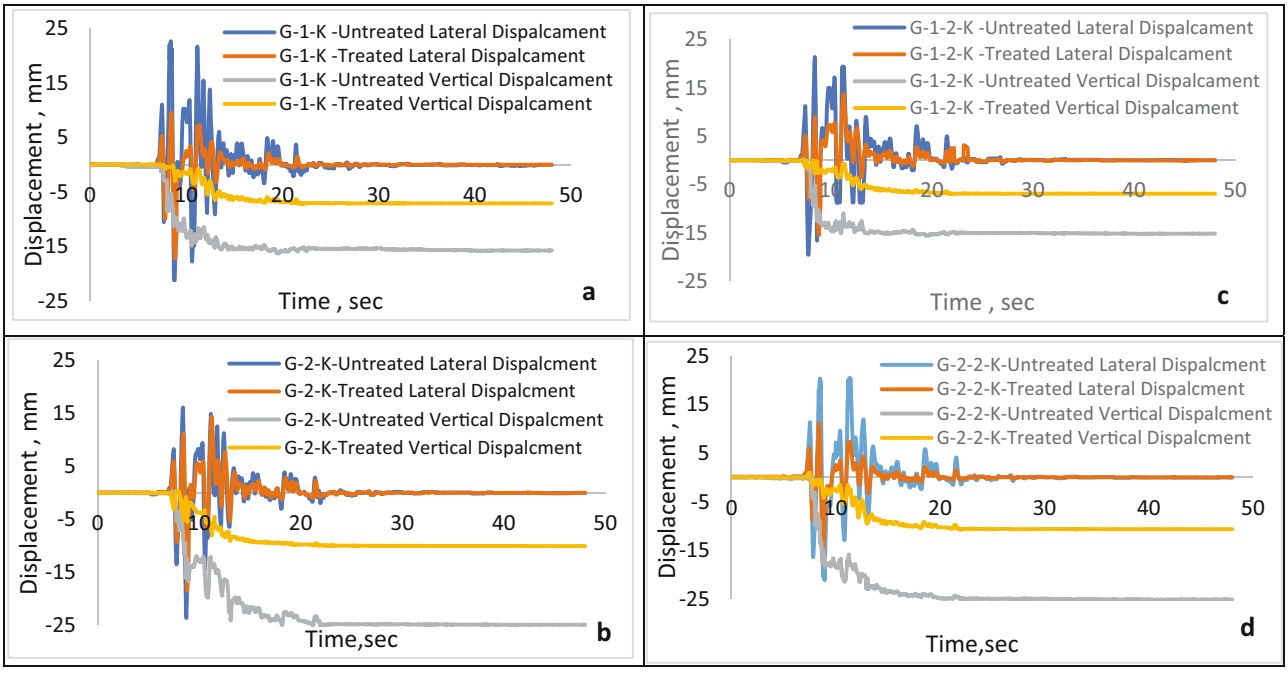

Figure 4: Vertical and lateral displacements of the pile group in the treated and untreated soil with nano-clay at (a) 50% axial load, (b) 100% axial load, (c) 50% axial load and 100% lateral load, and (d) 100% axial load and 100% lateral load.

vertical 15 to 7 mm and 25 to 10 mm at 100% axial loading for both G-2-K and G-2-2-K, showing a 53% and 60% reduction, respectively, compared to untreated soil.

The pile response resulting in the middle of treated soil in the shaking table using nano-SiO_2 with 1/50 is shown in Figure 5. With the effect of lateral loading, the liquefied layer around the pile group has shown that the lateral displacements were considered more pronounced for strong shaking motions, showing a surprising increase for the last case G-2-2-K, in which this movement will reduce from 21.59 mm in untreated soil to 14.70 mm in treated with nano-SiO_2. The overall pile lateral displacements in the treated layer were reduced by 30–35% for test cases G-1-K, G-1-2-K, G-2-K, and G-2-2-K when compared to the equivalent measured displacement for the untreated soil. However, due to strong motion, the vertical displacement suffers from soil distribution around the piles in the treated layer and beneath the pile in the untreated layer.

Figures 6 and 7 show the moment profiles of the group pile during strong earthquake motion of Kobe with 100% lateral loading and 50–100% axial loading embedded in treated and untreated liquefied soil with nano-clay. The peak bending moments on P1 and P2 varied linearly with depth within the liquefied and dense non-liquefied layers, suggesting that the liquefied layer was so weak that it did not appreciably contribute to the moments of their distribution along with the piles. So, the peak bending values occurred at the upper and lower boundaries of the liquefied and non-liquefied layers during the early part of the shaking, nearly at a depth of 0.75 L below the shaking table surface. As shaking continued, the moment value at the lower boundary of the liquefiable sand layer remained at the interface between the untreated and the treated liquefiable layers. This suggests that the treated soil with nano-clay around the pile with 100% lateral load has lowered the peak bending value on P1 at the interface boundary between the two layers to about 25% for 50% and 100% axial loading due to increases in cyclic strength for nanoparticles and decreases in imposed bending moments along with pile cap. At the same time, these values rounded to about 27% for the second row with the same loading.

The influence of permeation grouting within loosely liquefied soil that was laid on the upper portion of the shaking table using nano-SiO_2 on the developed bending along pile length is illustrated in Figures 8 and 9; the result indicated that the peak bending was slightly lower at the interface boundary when compared with nano-clay. The peak moments on P1 and P2 also occurred at the upper and lower boundaries between treated and untreated layers of 375 mm. The nano-SiO_2-treated layer enhances the neighboring soil, resulting in the measured moments of P1 within the leading row exhibiting a

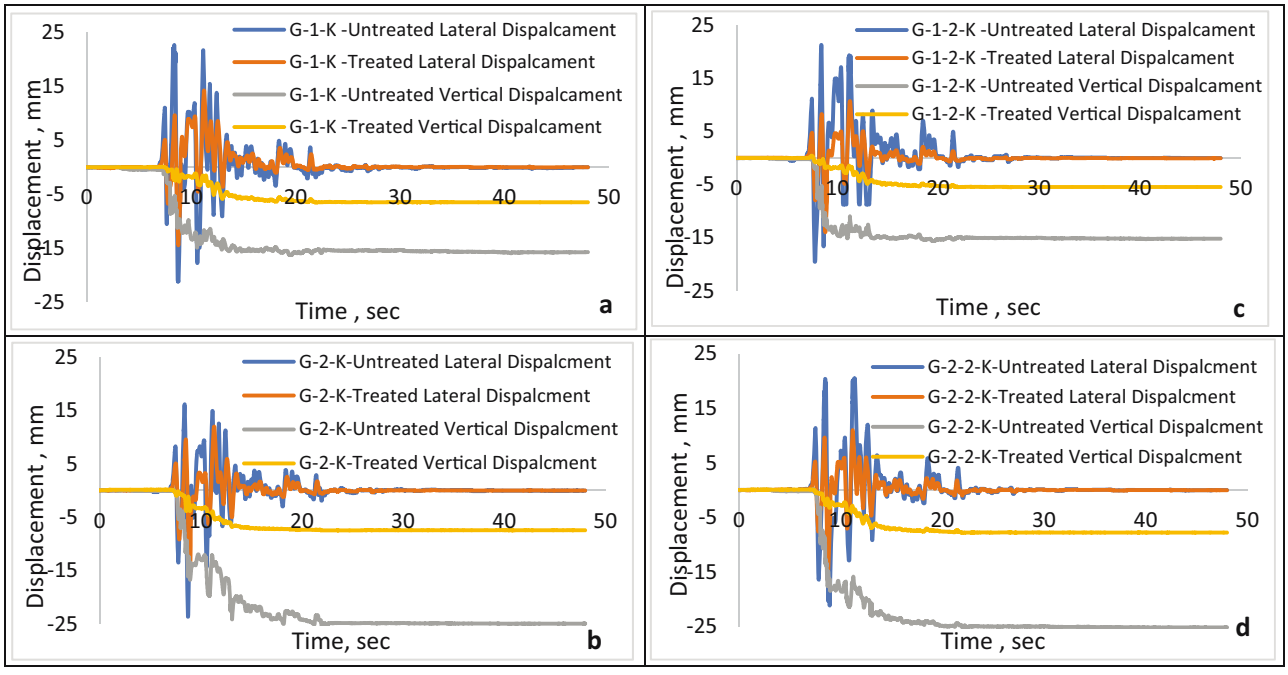

Figure 5: Vertical and lateral displacements of the pile group in the treated and untreated soil with nano-SiO_2 at (a) 50% axial load, (b) 100% axial load, (c) 50% axial load and 100% lateral load, and (d) 100% axial load and 100% lateral load.

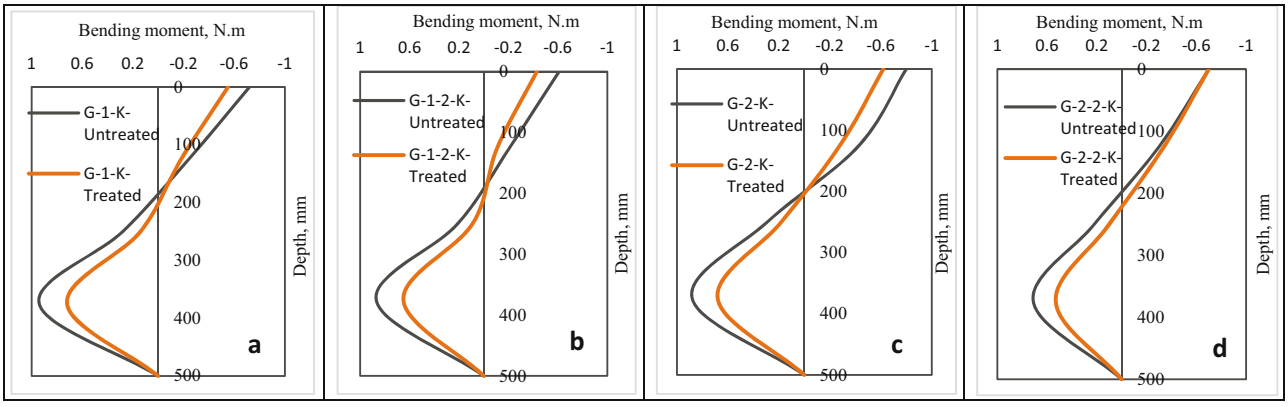

Figure 6: Bending moment of the pile group in the treated and untreated soil with nano-clay – P1 at (a) 50% axial load, (b) 50% axial load and 100% lateral load, (c) 100% axial load, and (d) 100% axial load and 100% lateral load.

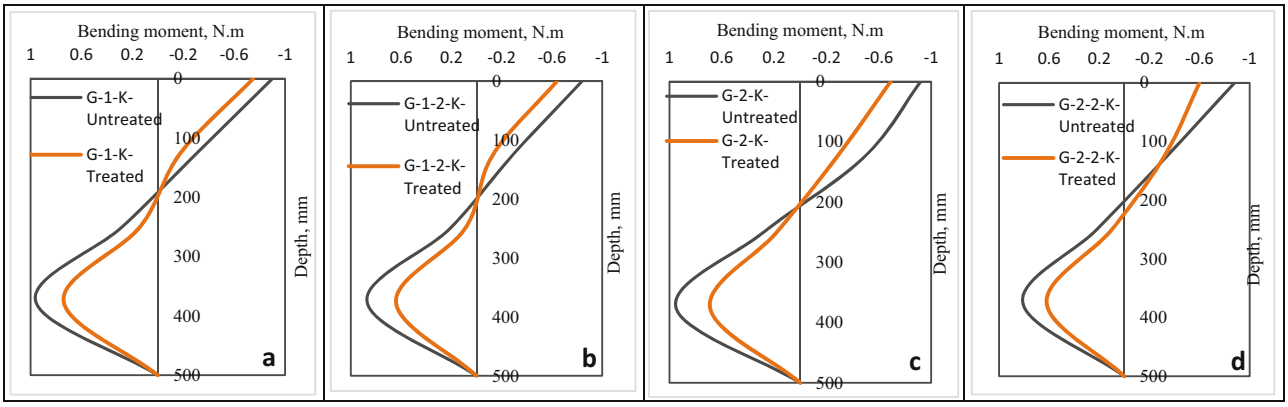

Figure 7: Bending moment of the pile group in the treated and untreated soil with nano-clay – P2 at (a) 50% axial load, (b) 50% axial load and 100% lateral load, (c) 100% axial load, and (d) 100% axial load and 100% lateral load.

reduced value ranging from 34 to 38% for increasing axial mass loading from 50 to 100%, respectively, at constant lateral loading of 100%.

Acceleration time histories ACC2 and ACC3 measured in the soil deposit of the shaking table at a depth of 120 and 220 mm are shown in Figure 10 for treated and untreated layers with nano-clay. The permeation grouting with nano-clay of the shaking table shows that the acceleration records in the near-field of ACC2 and ACC3 for the treated surrounding group of the pile in the upper sand

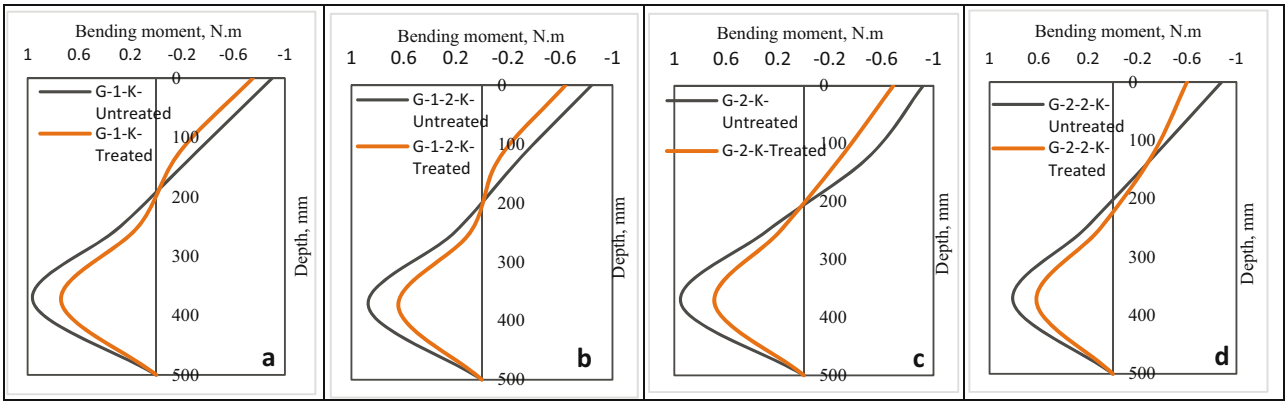

Figure 8: Bending moment of the pile group in treated and untreated soil with nano-SiO_2 – P1 at (a) 50% axial load, (b) 50% axial load and 100% lateral load, (c) 100% axial load, and (d) 100% axial load and 100% lateral load.

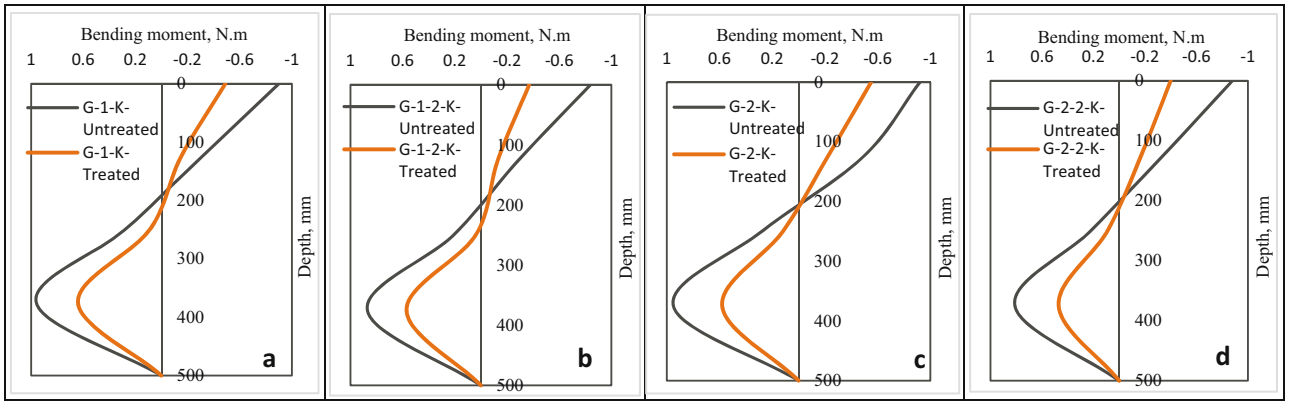

Figure 9: Bending moment of the pile group in treated and untreated soil with nano-SiO_2 – P2 at (a) 50% axial load, (b) 50% axial load and lateral load, (c) 100% axial load, and (d) 100% axial load and 100% lateral load.

layer have similar behavior to the measured input motions of the untreated layer except that the amplitudes were not symmetrical and exhibited large spikes in positive acceleration amplitude. At the same time, it dropped in the negative direction of shaking for all treated cases with nano-clay than for the untreated ones. This could indicate that the acceleration of the treated layer during shaking may be attenuated due to dampening related to the addition of nano-clay dispersion between sand particles.

The acceleration of the treated liquefied sandy layer with nano-SiO_2 is described in Figure 11. From these results, it can be shown that there is a drop in amplitude after several cycles during a strong Kobe earthquake. The magnitude of the accelerations ACC2 and ACC3 was noted to be reduced at the peak of the ground earthquake motion by about 30% for all test cases as compared to the untreated layer, and this scenario was attributed to the effect of nano-SiO_2, which plays an important role in the stiffening and cementation of tiny nanoparticles that tends to less dilative behavior of the nano-SiO_2-treated layer that remained solid after several cycles of shaking. The overall acceleration amplitude of the

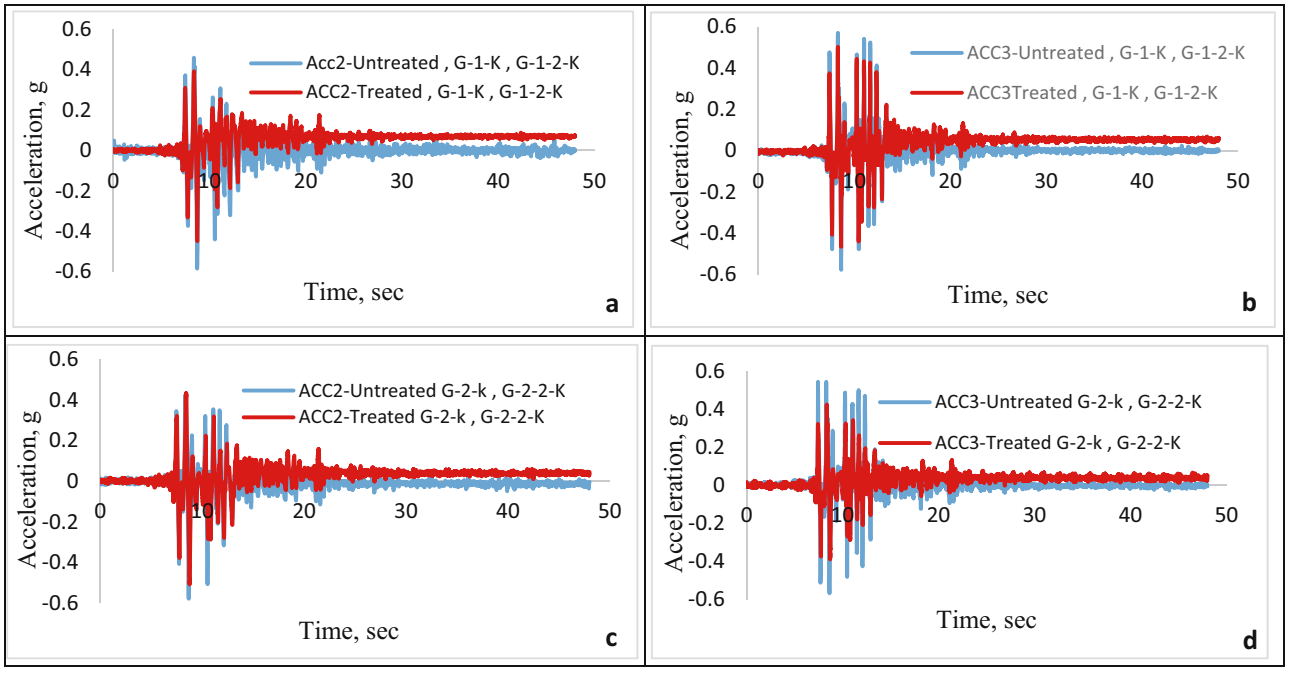

Figure 10: Acceleration within different depths of treated and untreated soil with nano-clay: (a and b) ACC2 and ACC3 at 50% axial load and 50% axial load and 100% lateral load; (c and d) ACC2 and ACC3 at 100% axial load and 100% axial load and 100% lateral load.

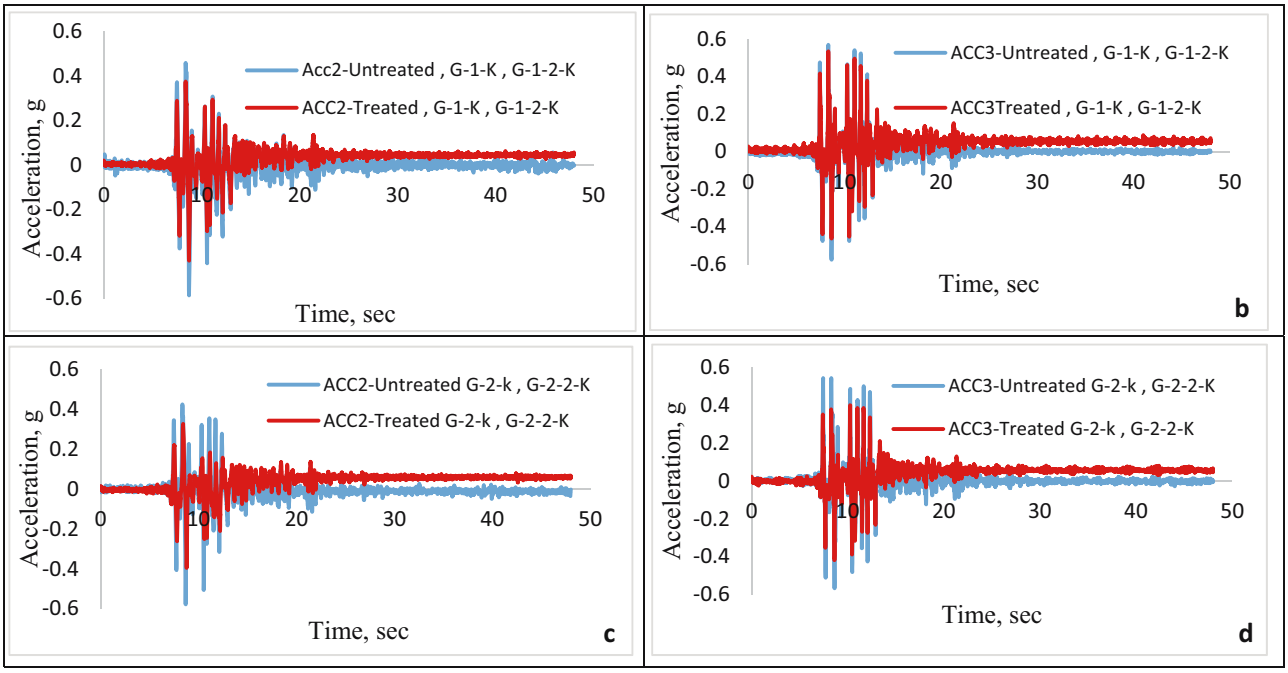

Figure 11: Acceleration within different depths of treated and untreated soil with nano-SiO_2: (a and b) ACC2 and ACC3 at 50% axial load and 50% axial load and 100% lateral load; (c and d) ACC2 and ACC3 at 100% axial load and 100% axial load and 100% lateral load.

treated layer with both nano types indicates that grouting with nano-SiO_2 experiences a slight effect over the nano-clay of the liquefied layer due to the stiffness and strength effect of tiny nano-SiO_2 that will solidify the layer after several cycles, and thus, the soil did not liquefy at the first shaking duration.

Figure 12 illustrates the values of the pore pressure ratio before and after treating the liquefiable layer with

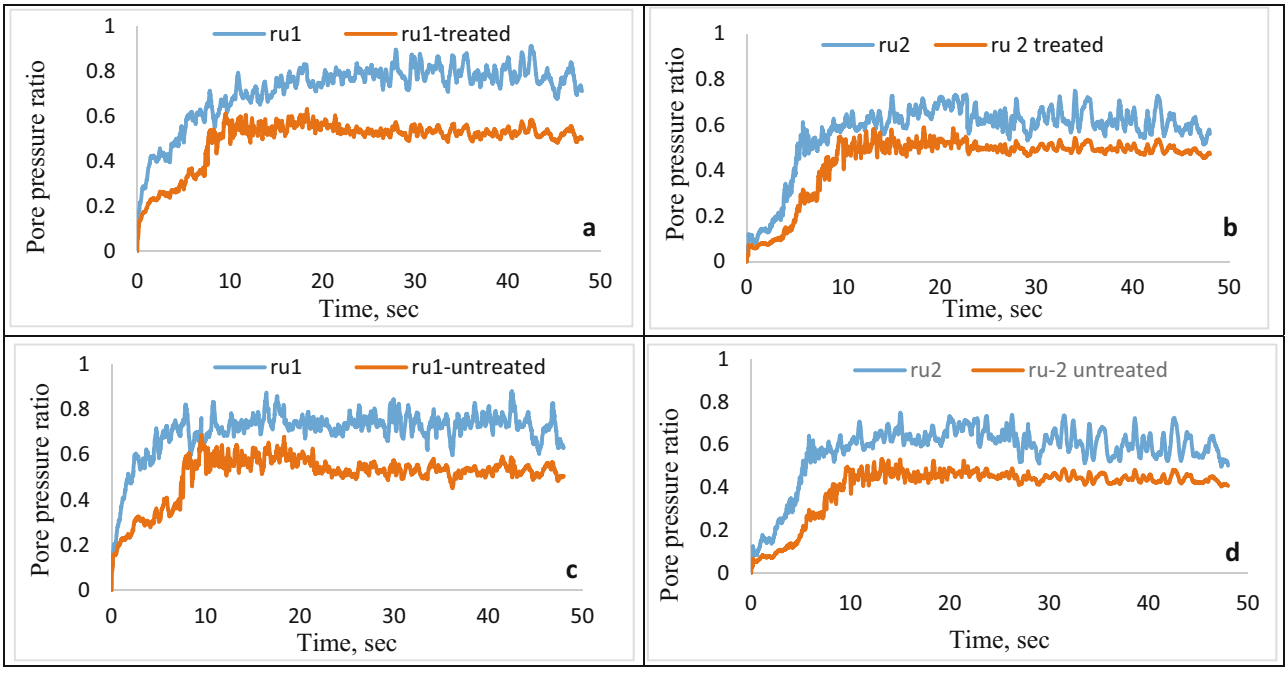

Figure 12: Pore pressure ratio within treated and untreated soil with nano-clay: (a and b) ru1- and ru2-treated at 50% axial load and 50% axial load and 100% lateral load; (c and d) ru1- and ru2-untreated at 100% axial load and 100% axial load and 100% lateral load.

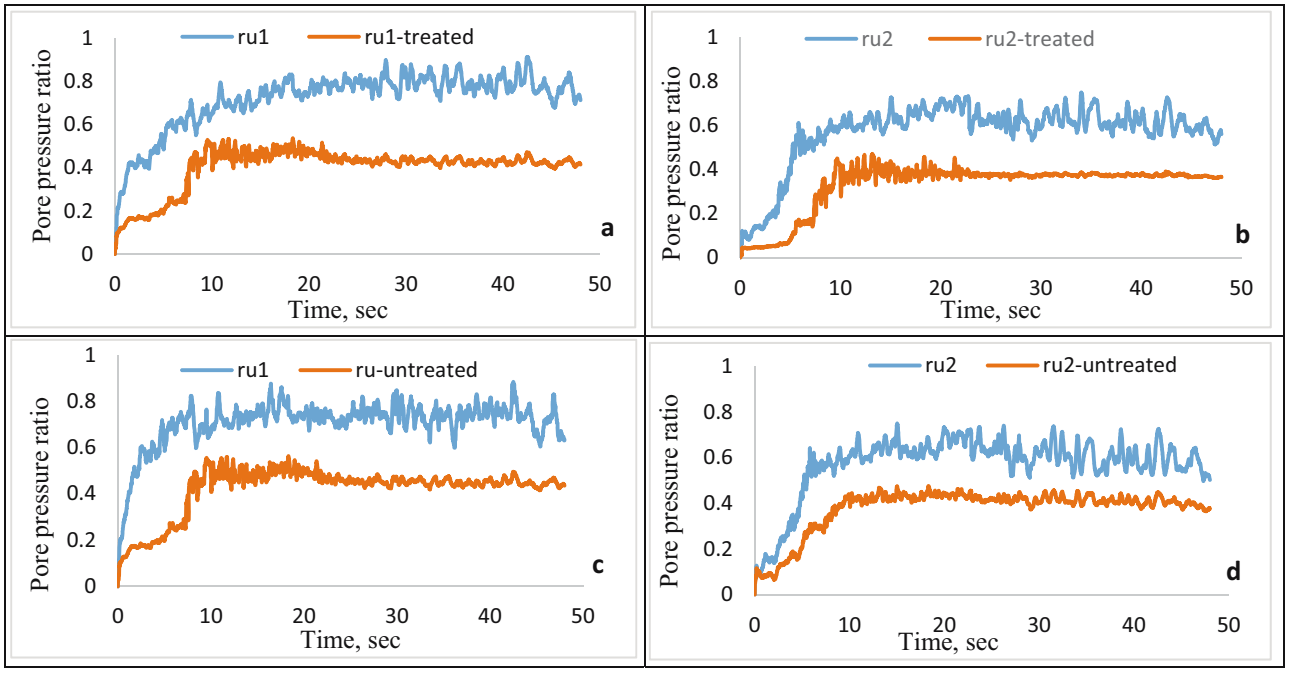

Figure 13: Pore pressure ratio within treated and untreated soil by nano-SiO_2: (a and b) ru1- and ru2-treated at 50% axial load and 50% axial load and 100% lateral load; (c and d) ru1- and ru2-untreated at 100% axial load and 100% axial load and 100% lateral load.

nano-clay. It can be seen that the pore pressure propagation rate for ru1 and ru2 was much lower for the treated layer with nano-clay than in the untreated layer; therefore, the pore pressure ratio for the treated layer gradually accumulated and reduced, reaching a maximum value of 0.65 and 0.5 at peak input motions corresponding to ru1 and ru2, respectively, as compared to that untreated with 0.88 and 0.74. However, the treated layer appears to have lagged behind the earthquake after reaching its peak value long after shaking ceased for about 9–10 s due to the influence of nano-clay in the form of a solid-like gel that does not entirely fluidize. Therefore, the pore pressure generation is delayed. Moreover, the peak values of ru1 and ru2 are lower in the treated layer than in the untreated one. This finding is similar to the results noted by refs [11] and [12].

The mechanisms of soil grouting by nano-SiO_2 to mitigate liquefaction potential are pore fluid solidification, soil grain cementation, and the delay of pore pressure generation. The influence appeared in Figure 13, indicating liquefaction resistance. The pore pressure accumulation process in the treated layer is delayed as presented in recorded values of ru1 and ru2, and the deformation of loose sands subjected to earthquake shaking is much smaller than that of the untreated layer. Also, it must be noted here that all treated and untreated soil will not experience a liquefaction potential since both r_u values will not reach 1 and indicate significant drainage away from the soil beneath the pile cap.

4 Conclusions

1. The reduced value of acceleration at pile cap has resulted from the contribution of the lateral loading effect, so the treated liquefied layer with both nano-material types had no effect on the measured acceleration at pile cap.
2. The treated soil did not liquefy and thus transmitted shear stresses through the surface induced by the base shaking. The overall acceleration amplitude of the treated soil layer shows the permeation grouting with nano-SiO_2 experiences a slight effect over nano-clay of the liquefied layer.
3. The inclusion of nano-materials with liquefied soil layer can delay the generation of pore water pressure during the Kobe earthquake by about 9–10 s due to the influence of nano-clay in the form of a solid-like gel that does not entirely fluidize.
4. The maximum bending moments along the pile were concentrated near or around the pile cap and interfaces between the liquefiable and non-liquefiable sand soil layers. The maximum moments were proportional to

the permanent lateral ground displacement. The treatment of liquefiable soil with nanomaterials reduced pile bending moments by 30% compared to the moment measured in the untreated model.

5. The lateral pile displacements in the treated soil layer were reduced by 30% for test cases compared to the equivalent measured displacement for the untreated soil, whereas the vertical displacement values of the treated soil displayed a reduction of nearly 50–60%, including 100% lateral loading for both nanomaterials.

Funding information: The authors state no funding involved.

Author contributions: All authors have accepted responsibility for the entire content of this manuscript and approved its submission.

Conflict of interest: Authors state no conflict of interest.

References

[1] Majeed Z, Taha M. A review of stabilization of soils by using Nano-materials. Australian J Basic Appl Sci. 2013;7(2):576–81.

[2] Albusoda BS, Almashhadany OY. Effect of allowable vertical load and length/diameter Ratio (L/D) on behavior of pile group subjected to torsion. J Eng. 2014;20(12):13–31.

[3] Huang C, Sui L, Wang K. Mitigation of soil liquefaction using stone columns: an experimental investigation. Mar Geo-Res Geo-Technol. 2016;34(3):244–51. doi: 10.1080/1064119X.2014.1002872.

[4] Çelik S, Negahdar A, Barough MJ. Effect of nano-particles on geotechnical engineering properties of granular soils by using injection method. J Biochem Tech. 2019;10(2):56–60. https://jbiochemtech.com/article/effect-of-nanoparticles-on-geotechnical-engineering-properties-of-granular-soils-by-using-injection-method.

[5] Sadiq AM, Albusoda BS. Experimental and theoretical determination of settlement of shallow footing on liquefiable soil. J Eng. 2020;26(9):155–64.

[6] Gallagher P, Mitchell J. Influence of colloidal silica grout on liquefaction potential and cyclic undrained behavior of loose sand. Soil Dyn Earthq Eng. 2002;22:1017–26.

[7] Boulanger RW, Idriss IM. Evaluating the potential for liquefaction or cyclic failure of silts and clays. Davis (CA), USA: Center for Geotechnical Modeling; 2004.

[8] AL-Kinani A. An apparatus for specimen preparation and testing of grouted soil [dissertation]. Baghdad: Al-Mustansirya University; 2011.

[9] Huissen RS, Albusoda BS. Numerical simulation of a single pile under the combined effects of axial and lateral loading in liquefiable soil. IOP Conf Ser: Mater Sci Eng. 2021;1067:012026.

[10] Hussein RS, Albusoda BS. Experimental and numerical analysis of laterally loaded pile subjected to earthquake loading. In: Karkush MO, Choudhury D, editors. Modern applications of geotechnical engineering and construction. Singapore: Springer; 2021. p. 291–303.

[11] Pamuk A, Gallagher P, Zimmie T. Remediation of pile foundations against lateral spreading by passive site stabilization technique. Submitted Soil Dyn Earthq Eng. 2007;27:864–74.

[12] Hiang C, Sui L, Wang K. Mitigation of soil liquefaction using stone column an experimental investigation. Mar Georesources Geotechnol. 2016;34(3):244–51.